Proceedings of IMECE2006:
2006 ASME International Mechanical Engineering Congress and Exposition
November 5-10, 2006, Chicago, Illinois, USA

IMECE2006-14575

VALIDATION OF A NEW ALUMINUM HONEYCOMB CONSTITUTIVE MODEL FOR IMPACT ANALYSES

Terry Hinnerichs
Sandia National Laboratories
tdhinne@sandia.gov
Albuquerque, NM 87185-0372

Eric Pulling
Sandia National Laboratories
epullin@sandia.gov
Albuquerque, NM 87185-0372

Mike Neilsen
Sandia National Laboratories
mkneils@sandia.gov
Albuquerque, NM 87185-0893

Wei-Yang Lu
Sandia National Laboratories
wlu@sandia.gov
Livermore, CA 94551-0969

ABSTRACT

A new constitutive model for large deformation of aluminum honeycomb has been developed. This model has 6 yield surfaces that are coupled to account for the orthotropic behavior of the cellular honeycomb being crushed on-axis and off-axis. Model parameters have been identified to fit uniaxial and biaxial crush test data for high density (38 lb/ft3) aluminum honeycomb. The honeycomb crush model has been implemented in the transient dynamic Presto finite element code for impact simulations. Simulations of calibration and validation experiments will be shown with model predictions compared with test data. Also, the honeycomb model's predictions will be compared with the older Orthotropic Rate Model predictions.

INTRODUCTION

Aluminum honeycomb is an excellent shock mitigation material for vehicle bumpers or shipping containers. It is generally orthotropic with three principal material directions that result due to its composition of corrugated and flat aluminum sheets. The directions, T the strongest, L the intermediate strength and W the weakest, are labeled in Figure 1.

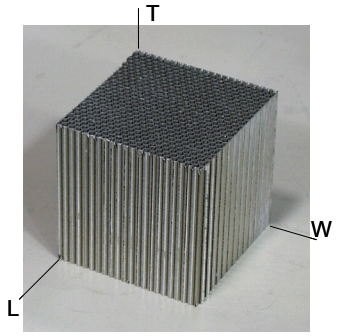

Figure 1. Aluminum honeycomb geometry and principal directions.

Earlier papers have described the on-axis behavior [1] and shear deformation behavior [2] of high density (38 lbs/ft^3) aluminum honeycomb, designated by Hexcel Corp. as CR-8-LC-1/8-5052-006-R2 [2]. These papers showed the test data compared with finite element predictions using an Orthotropic Crush Model (OCM) for the honeycomb. The OCM performs well for on-axis crush behavior but lacks the ability to follow off-axis crush and shear deformation behavior. Earlier papers introduced a new constitutive model, called the Honeycomb Crush Model (HCM), aimed at improving the ability to predict off-axis crush of aluminum honeycomb [5,6]. In these papers the calibration and validation processes were outlined. This paper will present

the results of completing the HCM calibration and validation processes. First a description of the experimental test procedure used for calibration and validation is given. Next experimental and model uncertainty is discussed. Finally, the model calibration and validation results are presented.

Experimental Procedure

Uniaxial and equal biaxial crush experiments were performed on high density aluminum honeycomb in the biaxial test rig shown in Figure 2a. The system provides in-plane loading in two perpendicular axes, i.e. East-West (EW) and North-South (NS) directions. There are four hydraulic actuators, two per each loading axis, and four control channels, which allow independent control of each actuator. A load cell is bolted to the end of each actuator. A biaxial compression fixture with a capacity of 40 kips is attached to each load cell through two bearing assemblies, which allow the fixture to move with the actuator in the loading direction while accommodating motion perpendicular to the loading direction in the loading plane. A sliding guide mechanism is mounted on each fixture plate to define and adjust relative position and motion between adjacent fixtures. It enables flexible loading paths. A close up view of a test setup is shown in Figure 2b where the test specimen is highlighted in red.

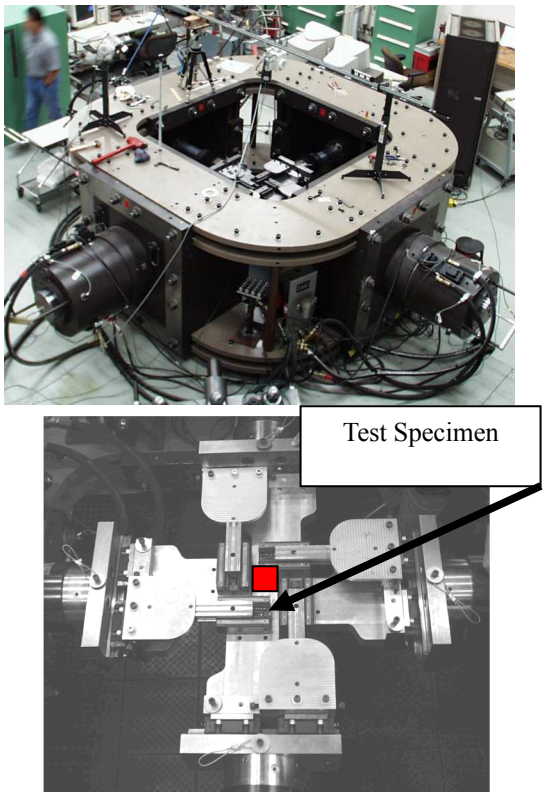

Figure 2. (a) In-plane biaxial system and (b) biaxial compression fixture at SNL/CA.

Figure 3a shows a convention for defining the biaxial test sample configurations. They are designated as XYθ, where X (or Y) represents the principal axis (i.e. T, L, or W) of the honeycomb, the XY plane is parallel to the loading plane, and θ is the angle between the material axis (X or Y) and the loading axis (EW or NS). Figures 3b and 3c give specific examples of using this convention. In Figure 3b the angle θ is zero for the TL00 configuration whereas in Figure 3c, θ is 45 degrees for the LW45 configuration.

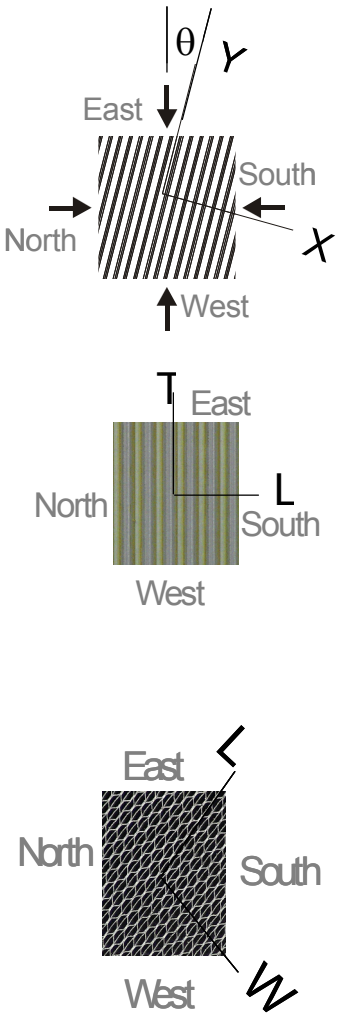

Figure 3. Examples of biaxial specimen configurations: (a) definition, (b) TL00, and (c) LW45.

In a series of tests conducted in this study, specimens were oriented in the TL00, TW00, LW00, TL45, LW45 and TW45 configurations. The nominal specimen size was 2.0” x 2.0” x 1.5”.

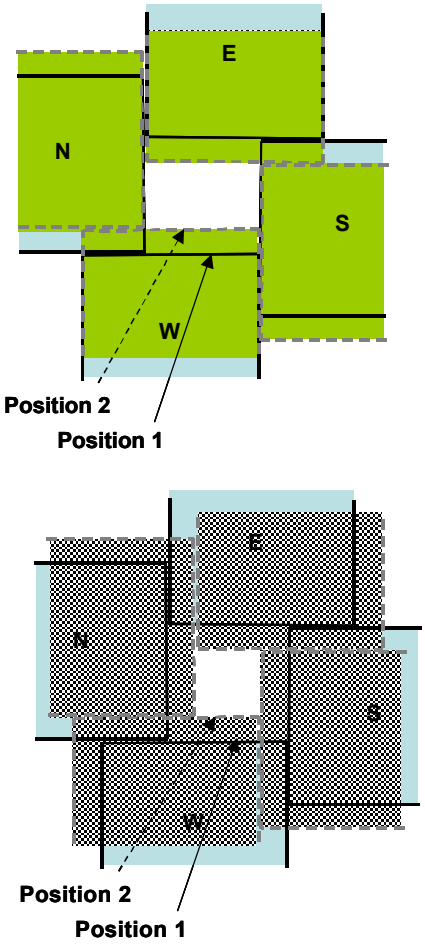

Figure 4. Uniaxial crush and equal biaxial crush on the biaxial system.

The experimental program involved two types of loading: uniaxial crush and equal biaxial crush. They are illustrated in Figure 4. During uniaxial crush on the biaxial system, the East and West actuators move toward each other at a constant speed 0.5 inch per minute, while the North and South actuator do not move and confine the deformation of honeycomb specimen. Both crush load and confined load were recorded. The remaining two faces that were normal to the loading plane were free. During equal biaxial crush, both East-West and North-South pairs of actuators moved toward each other. All other conditions were similar to the uniaxial crush test.

Additional uniaxial tests were performed with a fully confined rectangular chamber and piston setup, not shown. Here the nominal honeycomb sample cross section was 1.2" x 1.2" and 1.5" tall. This setup was the primary configuration for testing honeycomb but did not enable measuring the lateral stresses in the chamber.

Variation in the experimental data was due primarily to material variation. However, for the low transverse stress measurements, around 100 psi, friction contributes significant uncertainty to the load measurements [5].

Model Parameter Identification

The nine independent elastic constants, three Young's modulus values, three shear modulus values and three Poisson's ratios, were obtained from complementary cell level computational simulations and modal tests on the honeycomb [7]. This method was a hybrid experimental-numerical procedure where models were used to simulate tests and thereby extract estimates of the elastic constants. Basically the elastic constants in the model were calibrated until the predicted Eigen values matched the test data.

The orthotropic elastic constants determined for uncompacted 38 lbs/ft3 aluminum honeycomb are given in Table 1. Only 9 constants are independent; three of the Poisson's ratios depend on the other constants as described in [8]. Note that Poisson's ratio can be larger than 0.5 with an orthotropic material.

Table 1. Orthotropic elastic constants.

Parameter	value
Young's Moduli	(psi)
Ett	2.29E+06
Ell	1.18E+06
Eww	6.13E+04
Shear Moduli	(psi)
Gwl	4.18E+04
Glt	7.26E+05
Gtw	1.31E+05
Poisson's Ratios	
Vlw	1.489
Vtw	0.3307
Vwl	0.0774
Vtl	0.3291
Vwt	0.0089
Vlt	0.1698

Table 2 lists the isotropic elastic properties that were used to represent the honeycomb near its lockup strain of 0.78. The modulus value assumes imperfect compaction so that the full modulus of solid aluminum is not achieved.

Table 2. Isotropic elastic properties.

Parameter	value
Young's Modulus	psi
E	4.00E+06
Poisson's Ratio	
V	0.3

A somewhat similar approach to the above hybrid experimental-numerical approach was used to identify the form of the model and parameters governing the plastic deformation. Non-homogeneous deformation in the form of a crush front propagating through the material occurs during

the compaction tests on aluminum honeycomb. Consequently, each calibration test configuration was modeled and simulated to define the HCM form and quantify the model parameters that would minimize the differences between model predictions and test data. The nonlinear transient dynamic finite element code called Presto was used for these simulations [9].

A matrix of biaxial and uniaxial crush tests were identified that would provide data to quantify each of the HCM parameters and tabular functions [10]. Table 3 lists the complete matrix of calibration tests that were conducted. Three replicates were done for each test condition to quantify unit-to-unit variability in the specimens. As shown in the Temperature column of Table 3, there were some tests performed at ambient and at 165 deg F. Only some configurations that included the strong T-direction were tested at the high temperature.

Table 3. Calibration Test Matrix.

Test Rig	Type of Load	Orientation	Temperature	Model Parameter or Function Defined
biaxial system	uniaxial with inplane confinement	TL00	ambient & 165 F	TTP, HT, TS, b_1
"	"	TW00	ambient	TTP, HT, TS, c_1
"	"	LW00	"	LLP, H_L, LS, c_2
"	"	TW45	ambient & 165 F	TWS, mu
"	"	LW45	ambient	LWS
uniaxial chamber	uniaxial with full confinement	TL45	ambient & 165 F	TLS
"	"	WT00	ambient & 165 F	WWP, WS, H_W
biaxial system	equal biaxial with inplane confinement	TL00	ambient	E_{stl}, E_{slt}
"	"	TW00	"	E_{stw}, E_{swt}

The column in Table 3 entitled "Model Parameter or Function Defined" lists the various parameters or tabular functions of the HCM that will be defined by the associated test on the same line. For example, the normal crush strength in the T-direction, TS, will be quantified based on simulating the TL00 test called out in the top line of Table 3.

Figure 5 shows the finite element model used to simulate the uniaxial and biaxial crush tests. The center square (red) mesh represents the honeycomb sample and the surrounding rectangular meshed parts represent the platens of the biaxial test rig. The platens are modeled as rigid bodies that have contact surfaces with the honeycomb.

Physical Length Scale and Mesh Convergence

A 20 x 20 x 1 mesh is used to model the 2" x 2" x 1.5" honeycomb sample. The element size for modeling the honeycomb of 0.1 inch was chosen since this is approximately the size of a unit cell (largest repeating geometric shape for the 38 lbs/ft3 honeycomb). The 0.1 inch element enabled the integration of a physically based length scale into the model since the physical honeycomb tends to crush one layer of cells at a time.

For computational efficiency, the platens were each given velocity components of 100 in/sec clockwise and inward to simulate the quasi-static biaxial crush experiments. Inertial effects for this Presto model were considered negligible at this rate. Contact forces calculated by the Presto code between the simulated platens and the honeycomb were collected, divided by the original area, and output for direct comparison with the experimental, engineering crush stresses. Figure 5b shows a partial crush of the TW45 configuration and the volumetric strain is color coded; red is low strain and blue is high. The model accurately predicted the orientation and location of the localized deformation that was observed experimentally.

Model Uncertainty

Sources of model uncertainty include, but are not limited to: (1) the functional form for the HCM, and (2) parameter values for a given functional form. The analytic hardening functions described in [6] are an example of the former, and any uncertainty in the yield strength of the material is one example of the latter. The model form consists of analytic functions and tabular functions. The analytic functions of the model will be held constant during the calibration process.

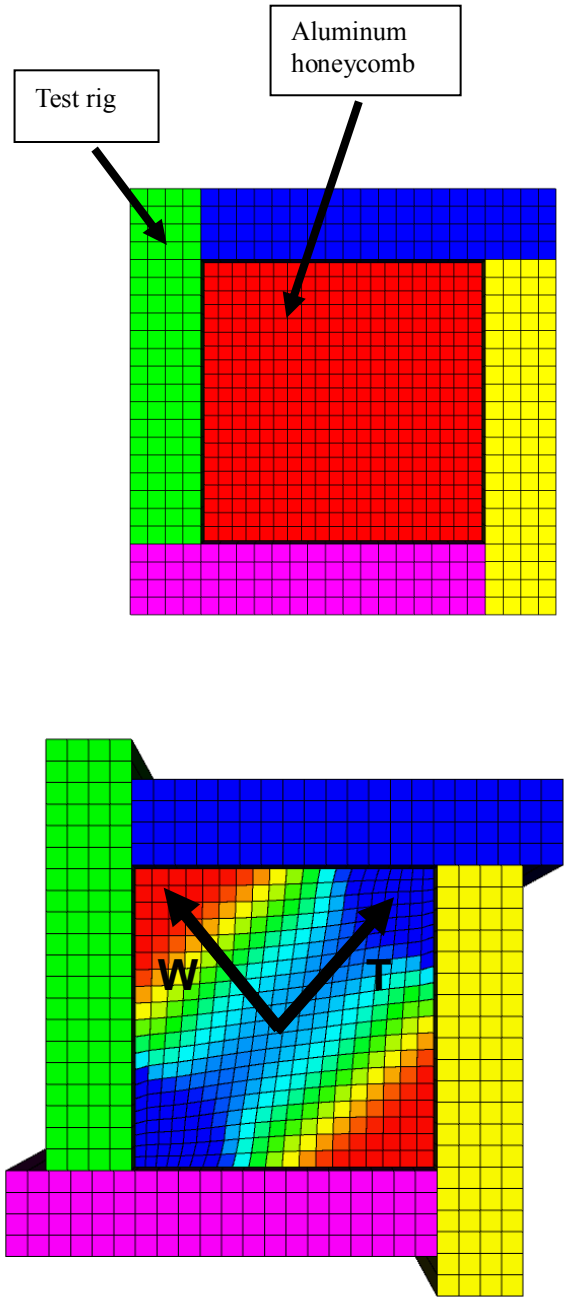

Figure 5. Finite element model for equal biaxial crush: (a) undeformed and (b) partially deformed TW45 configuration (volumetric strain is color coded).

The parameters associated with the analytic functions and the tabular functions were chosen for best fit with the calibration data and treated as deterministic. Only the initial yield strength values, (TS, LS, WS, TLS, LWS, WTS) were treated as random variables and their distributions are based on the calibration tests.

Additional model uncertainty is involved with the coefficient of friction between the platens and the honeycomb. The two values, 0.22 and 0.3, were used in the model. The lower value of friction was based on results from a test that measured frictional forces on a piece of 38 lbs/ft3 honeycomb rubbing on a steel plate [10]. The interface between the steel and the honeycomb for the friction test was lubricated similar to how the platens were lubricated in the biaxial calibration tests. The upper value of friction, 0.3, was chosen to quantify the sensitivity to friction in case the lubrication varied in the calibration tests.

Calibration and Validation Metric

One measure of how appropriate a model is for a shock mitigation device is its ability to predict the amount of energy absorbed by the device during an impact. For this reason, the metric chosen for determining the goodness of fit between model and test data will be based on strain energy density. For one-dimensional strain, the validation metric is given by Equation 1.

$$E_{metric}(\varepsilon_{max}) = \int_0^{\varepsilon_{max}} \sigma \cdot d\varepsilon \qquad \textbf{(Eq. 1)}$$

where σ is the engineering stress component in the loading or transverse direction, e.g. T or W, ε is the engineering strain in the loading direction, ε_{max} is the upper strain limit of the integral. Equation 1 is an integral measure that will factor in the general shape and the area under the stress-strain curves. This energy metric is used to compare energy absorbed in the model and the test data. Being an integral measure, it smoothes the model and test data making it easier to compare the two.

The calibration process involved performing multiple simulations of a given test configuration to quantify its sensitivity to a given parameter. Figure 6 shows the results of applying the process to the TL00 uniaxial strain test. In this case, the T-direction crush strength, TS, is varied in effort to determine the best fit. The coefficient of friction between the platens and the honeycomb, mu, is also varied to examine how much influence it has on the calibration process. Figure

6a shows the engineering stress in the T-direction plotted versus the engineering strain in the loading direction. Test data gathered from three independent tests for each configuration are shown.

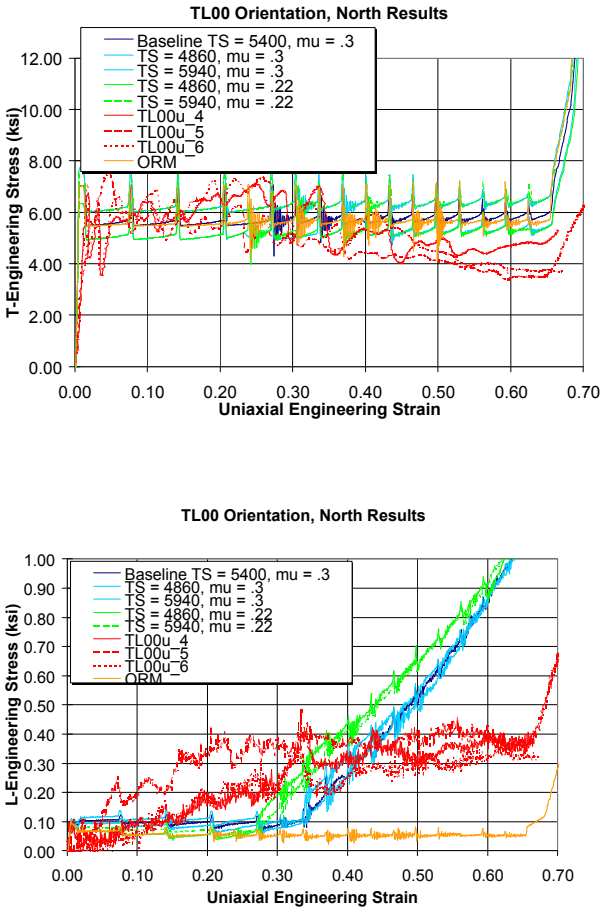

Figure 6. Model fit versus test data for TL00 uniaxial strain and sensitivity to TS and mu: (a) T-direction, (b) L-direction.

The HCM brackets the test data very well out to approximately 0.3 strain where the test data begins to drop off. The drop in T stress values for the test was due to the honeycomb greatly expanding out of plane due to splitting in the weak W-direction. The model can not account for gross splitting of the honeycomb and this phenomenon is less likely to happen with confinement in all directions. Figure 6b shows the engineering stress buildup in the L-direction which is transverse to the loading direction. Here the fit is not as good as the loading direction fit but the lateral stresses are ten times smaller than the T direction stress. Also, uncertainties in load measurement as discussed earlier and uncertainties in the initial clearance between the honeycomb and loading platens cause scatter between model and test.

Figure 7 shows the application of the energy metric from Equation 1 applied to the data in Figure 6. The curves are much smoother by using this metric. It was concluded from Figure 7 and similar data from the TW00 test, that the best fit value for TS was 5400 psi. The ORM results look similar to the HCM results for the T-direction but the L-direction stresses diverge from the test data for large strains.

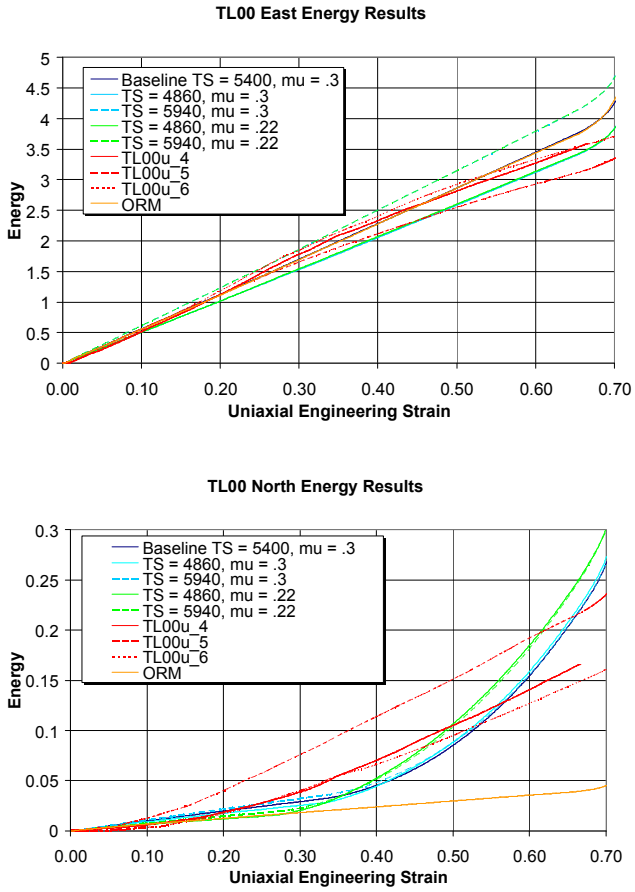

Figure 7. Model fit versus test data using the energy metric for TL00 uniaxial strain and sensitivity to TS and mu: (a) T-direction, (b) L-direction.

Figure 8 is similar to Figure 6 except that the sensitivity to the b_1 parameter and friction is being displayed. The only noticeable sensitivity to b_1 is displayed in the L-stress plot in Figure 8b. Also, the influence of friction is small compared to the changes due to b_1

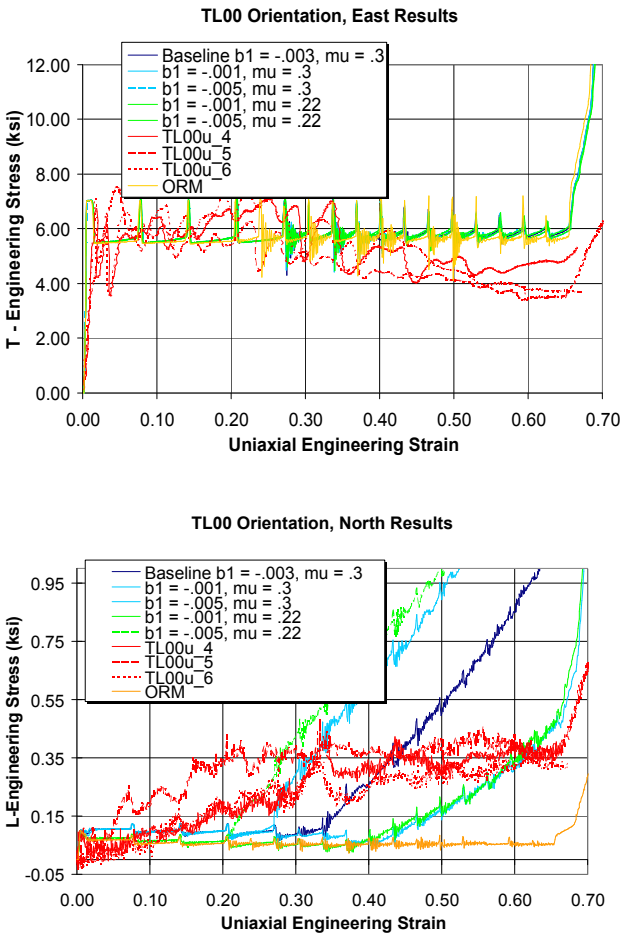

Figure 8. Model fit versus test data for TL00 uniaxial strain crush and sensitivity to b_1 and mu: (a) T-direction, (b) L-direction.

Figure 9 shows the sensitivity to the b_1 parameter and friction in the form of the energy metric, Equation 1. From Figure 8 and Figure 9 it was concluded that the best fit value for b_1 is -0.003 and that either value for friction works similarly.

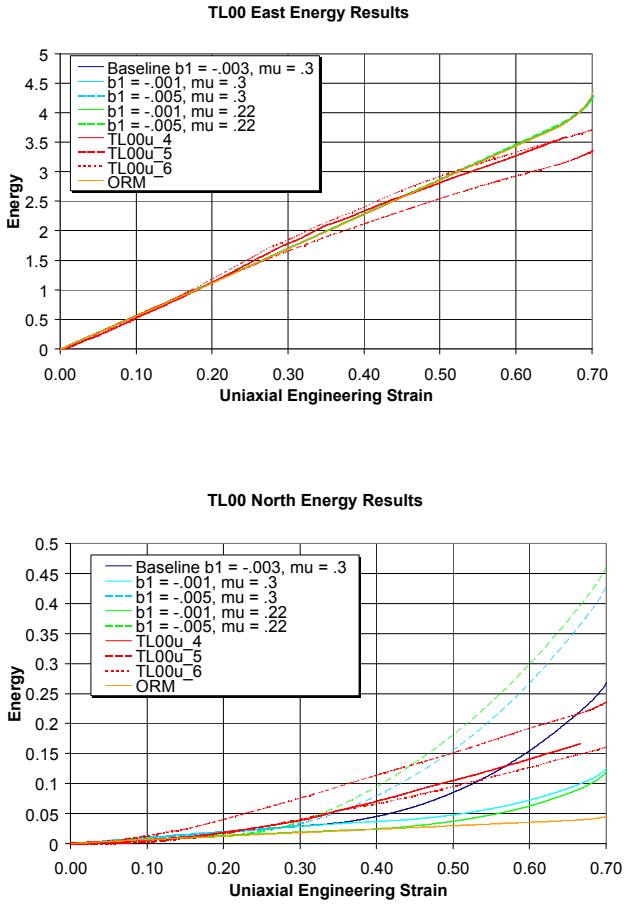

Figure 9. Model fit versus test data using the energy metric for TL00 uniaxial strain and sensitivity to b1 and mu: (a) T-direction, (b) L-direction.

This same approach of curve fitting with the energy metric to quantify the other HCM parameters was applied to the other calibration test data and model results, but it is not shown here. All of the material parameters for the new honeycomb crush model are summarized in Table 4. As mentioned earlier, only the normal and shear strengths will be treated as random variables and the other parameters will be single best fit values from the calibration process.

Table 4. Honeycomb Crush Model Calibrated Material Parameters.

Parameter	Value	Description of Parameter
A1, A2, A3	1.0, 0.0, 0.0	Coupling parameters for TT yield surface
B1, B2, B3	-.001, 1.000, 0.000	Coupling parameters for LL yield surface
C1, C2, C3	-.020, -.015, 1.000	Coupling parameters for WW yield surface
TS (psi)	5400 +/- 10%	Initial strength parameter for TT yield surface
LS (psi)	850 +/- 10%	Initial strength parameter for LL yield surface
WS (psi)	600	Initial strength parameter for WW yield surface
TLS (psi)	1200 to 1800	Initial strength parameter for TL yield surface
LWS (psi)	400 to 850	Initial strength parameter for LW yield surface
WTS (psi)	700 to 1150	Initial strength parameter for WT yield surface
ESTL	1.2	Hardening in T due to L strain
ESTW	2	Hardening in T due to W strain
ESLT	0	Hardening in L due to T strain
ESLW	-0.7	Hardening in L due to W strain
ESWT	4	Hardening in W due to T strain

The plus or minus 10% range for the TS and LS values was chosen based on the material specifications for manufacturing the honeycomb. Whereas, the values for the shear strengths, LWS and WTS, were a compromise best fit between the East and North curves measured in the biaxial rig for the uniaxial tests LW45, TW45. The range of values for TLS was determined based on the uniaxial chamber test, TL45, which only had measurements in the loading direction. Here the best fit value was expanded to include a 30% variation similar to the other shear components but limited to avoid any significant change deformation patterns from those observed in the tests [1].

The shear strength values (TLS, TWS, and LWS) determined by the calibration process are significantly lower than the vendor, Hexcel Corp. [2] publishes for undeformed honeycomb. However, the values reported here represent a best fit value over a large range of deformation where the shear strength dramatically decreases. Surprisingly, for this batch of aluminum honeycomb, the temperature effect was negligible. The ambient test data curves have similar scatter to the hot test data with no systematic offset. Consequently, these model parameters apply for ambient to 165 deg F conditions.

Model Validation

Validation predictions were made with the HCM and the finite element mesh shown earlier. The HCM parameters defined in Table 4 were used to predict the behavior of experiments defined in the validation test matrix given in Table 5. The tests chosen for validation in Table 5 are all off-axis tests and were chosen to quantify the predictive accuracy of the HCM where it is thought to be least accurate and for a configuration that is important to the system application. Also, note that the TW20 test configuration is listed both in the biaxial system and the confined chamber parts of the test matrix. This was planned in order to quantify differences between the biaxial system with one free direction and the chamber with full confinement.

To factor in the uncertainty of the honeycomb strength upper and lower bound values of the parameters in Table 5 were used in the HCM to predict an envelope of responses to correlate with the scatter of the test data. All of the strength values were considered to be strongly dependent so the highest value for each strength parameter was used for the upper bound calculation and the lowest value for each strength parameter was used for the lower bound calculation. The energy metric, given in Equation 1, was used for the calibration and also as a validation metric to quantify the difference between model predictions and test results.

Validation predictions were also made with the ORM model using one set of parameters that relate to the average values used in the HCM.

Table 5. Validation Test Matrix.

Test Rig	Type of Load	Orientation	Temp
biaxial system	uniaxial with inplane confinement	TW20	ambient
"	"	LW20	"
uniaxial chamber	uniaxial with full confinement	TL20	ambient
"	"	TW20	"
biaxial system	equal biaxial with inplane confinement	TL45	ambient
"	"	TW45	"
"	"	LW45	"

Model Predictions Correlated with Test Data

Figure 10 through Figure 16 show plots of the HCM predictions for each of the validation experiments listed in Table 5 along with the three test curves in each case. Each figure has two plots. Figure "a" on the left has engineering stress for the vertical axis and figure "b" on the right has the energy metric for its ordinate. In addition, a single curve is given for the ORM. The key question to answer for model validation is how well does the envelope predicted by the model overlap with the experimental envelope?

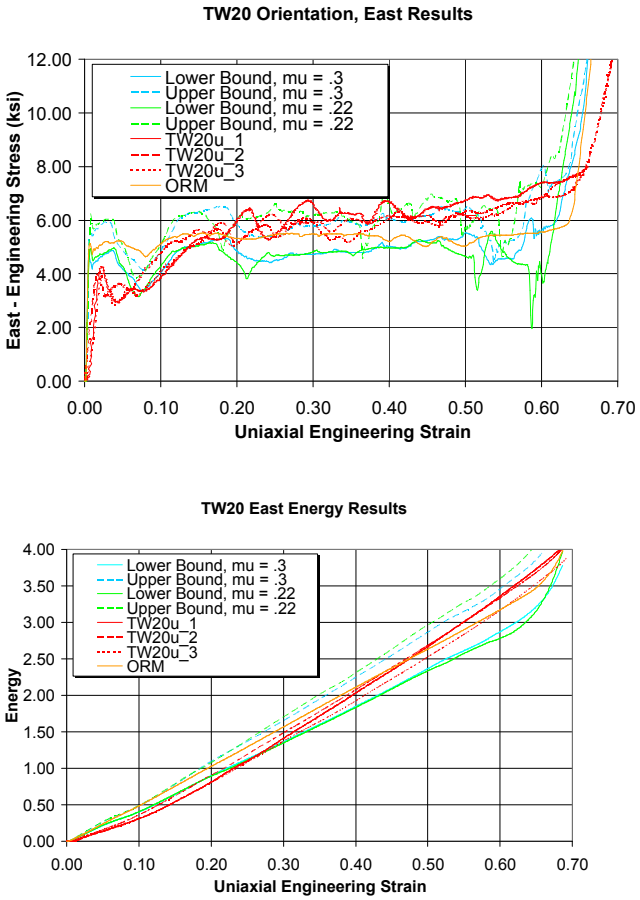

Figure 10. HCM and ORM Model fit versus test data for TW20 uniaxial crush: (a) East-direction stress, (b) East-direction energy metric.

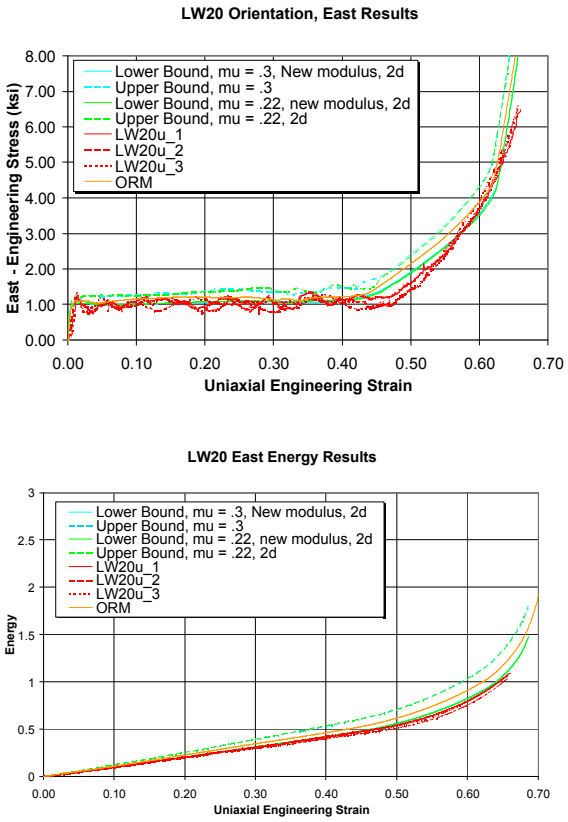

Figure 11. HCM and ORM predictions versus test data for LW20 uniaxial crush using the energy metric; (a) East-direction stress, (b) East-direction energy metric.

Model Validity

The criterion for determining if the model is valid was based on the amount of overlap that the model predicted energy envelope had with the experimental energy envelope at three locations along the strain axis. Our earlier paper [5] defined this process in more detail and specified the three strain points at which the experimental energy curves were at E/3, 2E/3, and E where E is the total energy metric at the final strain value. The final strain values chosen were 0.6 for the uniaxial tests and 0.4 for the equal biaxial tests. These equate to approximately the same volumetric strain values.

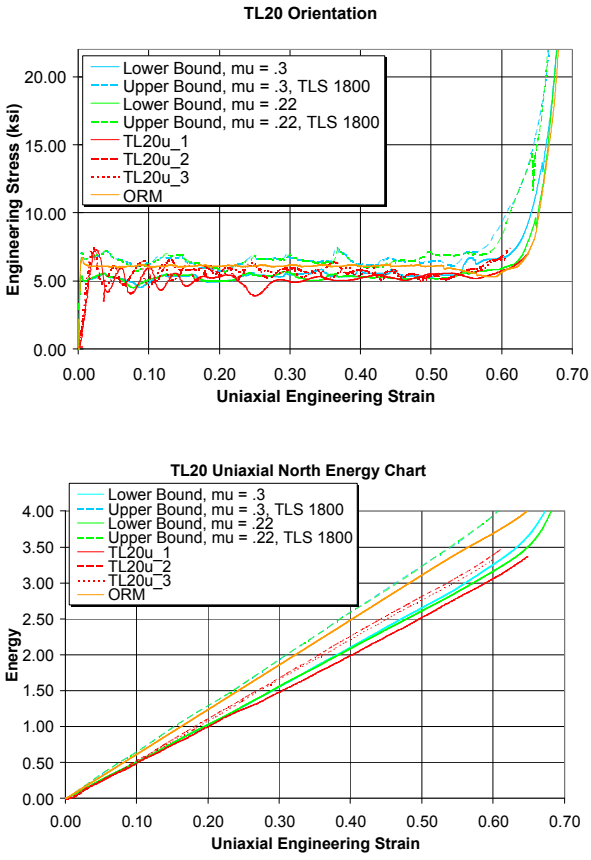

Figure 12. HCM and ORM predictions versus test data for TL20 uniaxial chamber crush; (a) Stress, (b) Energy metric.

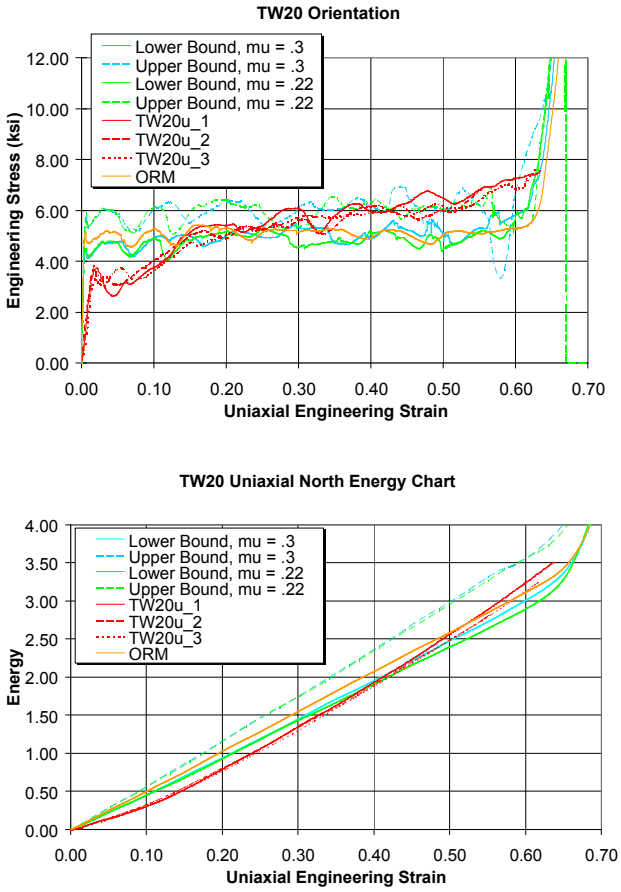

Figure 13. HCM and ORM predictions versus test data for TW20 uniaxial chamber crush; (a) Stress, (b) Energy metric.

Table 6 lists the amount that the model overlaps with the test data energy envelopes. Out of the 21 sample points (seven loading conditions and 3 energy levels per test), the model is overlapped 100% by the test data envelope in 11 cases. In the three LW20 cases the test data has a very narrow envelope that is tangent to the model's envelope. Somewhat similarly, in the three LW45 cases the model has a very narrow envelope that is tangent to the lower bound of the test data. But the north data (not shown) from the LW45 case overlaps on the high side of the experimental envelope. For all tests involving the T-direction, which has the highest strength, the model overlapped by 60% or greater for the two highest energy columns. The worst case of non-overlap was the TW20 chamber results in the E/3 column; which is mitigated by the 100% overlap recorded for the similar TW20 biaxial system test.

The model is validated subject to the limitations discussed herein for quasi-static uniaxial and biaxial crush deformations.

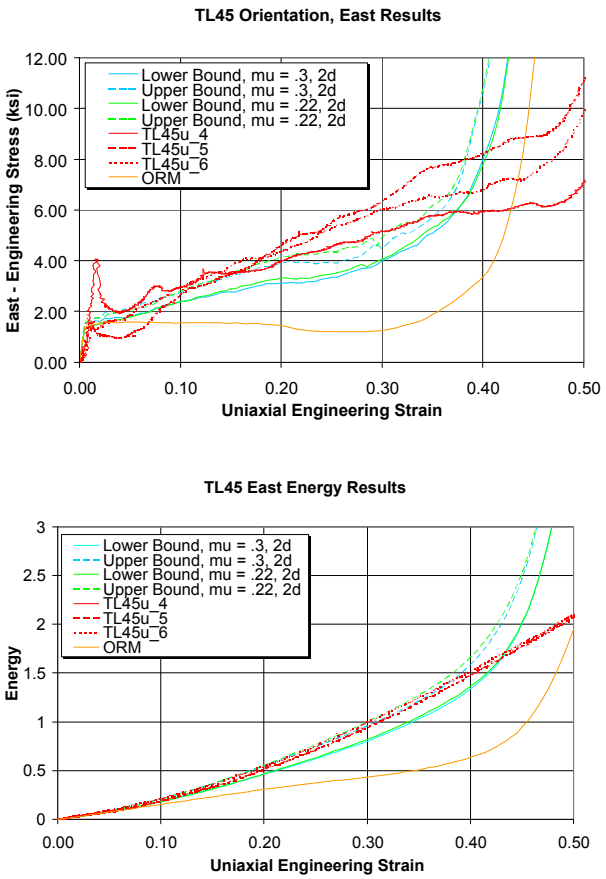

Figure 14. HCM and ORM Model fit versus test data for TL45 equal biaxial crush: (a) East-direction stress, (b) East-direction energy metric.

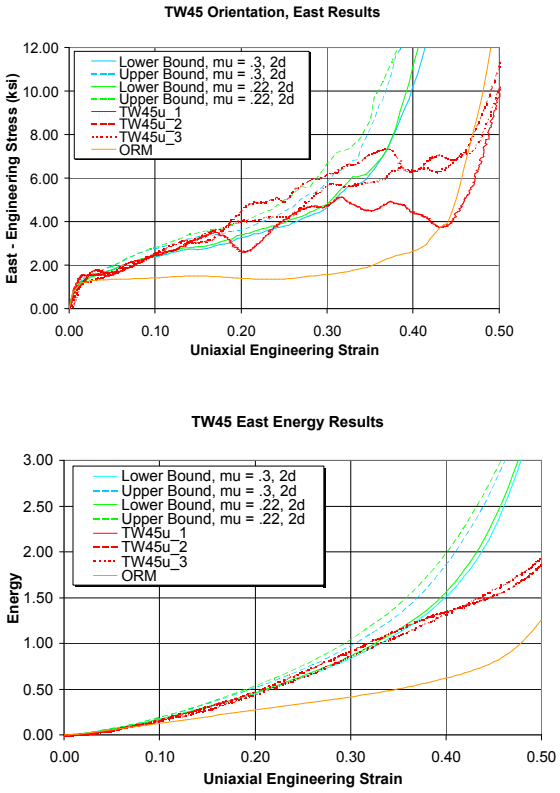

Figure 15. HCM and ORM Model fit versus test data for TW45 equal biaxial crush: (a) East-direction stress, (b) East-direction energy metric.

.

SUMMARY AND CONCLUSIONS

The validation process for the Honeycomb Crush Model (HCM) was presented. This included a parameter identification process based on a combined experimental/numerical approach of modeling and simulating biaxial crush tests and adjusting the parameters to minimize differences between the model and the test data. An energy metric was used to determine best fits for the calibration process and for the validation. Validation procedures included the effects of experimental and modeling uncertainty. Predictions using the calibrated HCM were presented for off-axis crush tests and compared with the validation test data and predictions using the Orthotropic Rate Model (ORM). The HCM demonstrated improvements over the ORM in predicting crush forces in equal biaxial loading situations. However, for most other uniaxial loading experiments the HCM results are similar to the ORM results.

For further improvements, combined compression/shear tests could be performed to better quantify the coupled strain softening of the shear and normal crush strengths. Information from these tests could be incorporated into the HCM for some of the functions that were left undefined, e.g. $TTLP(e_{tl})$ and $TLTLP(e_{tl})$.

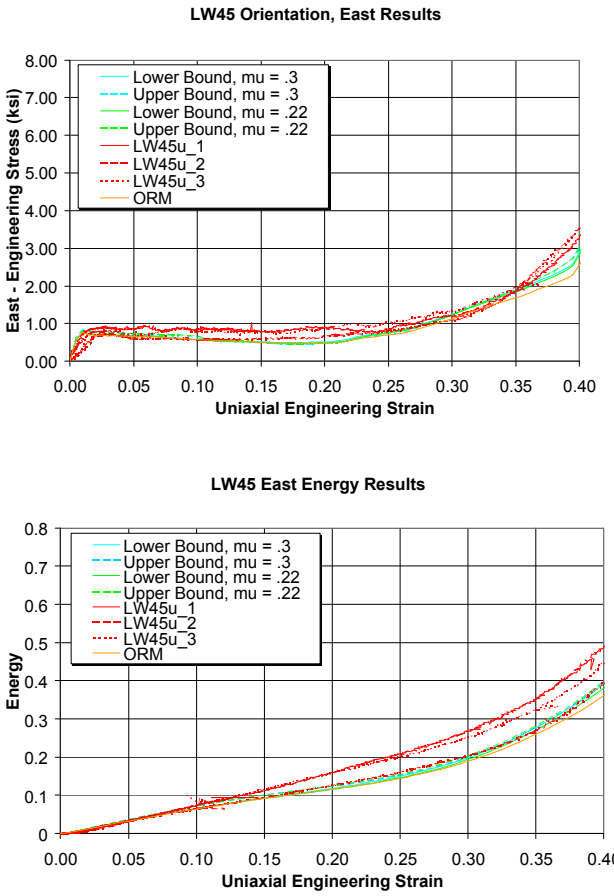

Figure 16. HCM and ORM predictions versus test data for LW45 equal biaxial crush stress; (a) East-direction stress, (b) East-direction energy.

Table 6. Model Validation Results.

Test Rig	Type of Load	Orientation	Model Overlap on Test Data, %		
			E/3	2E/3	E
biaxial system	uniaxial strain	TW20	100	100	100
"	"	LW20	0 *	0 *	0 *
uniaxial chamber	uniaxial strain	TL20	100	60 high	70 high
"	"	TW20	0	100	100
biaxial system	equal biaxial	TL45	100	100	100
"	"	TW45	100	100	0
"	"	LW45	0 #	0 #	0 #
* Narrow test data envelope is tangent to lower bound of model predicted enevelope.					
# Model predicted envelope is narrow and tangent to lower bound of test data envelope.					

ACKNOWLEDGEMENTS

We would like to thank Bill Scherzinger and Tom Carne for their technical support and advice. Sandia is a multiprogram laboratory operated by Sandia Corporation, a Lockheed Martin Company, for the United States Department of Energy's National Nuclear Security Administration under contract DE-AC04-94-AL85000.

REFERENCES

1. Lu, W.-Y. and Hinnerichs, Terry, "Crush of High Density Aluminum Honeycombs," IMECE/AMD-25453, 2001.
2. Lu, W.-Y., Korellis, J., and Hinnerichs, Terry, "Shear Deformation of High Density Aluminum Honeycombs", IMECE/AMD-44092, 2003.
3. "Mechanical Properties of Hexcel Honeycomb, "TSB-120, Hexcel Corporation, Dublin, CA, 1992.
4. Whirley, R.G., Engelman, B.E., and Hallquist, J.O., 1991, "DYNA3D Users Manual," Lawrence Livermore Laboratory, Livermore, CA.
5. Hinnerichs, Terry, Neilsen, M. Lu, Wei-Yang, "A New Honeycomb Constitutive Model for Impact Analyses", IMECE2004-60751.
6. Hinnerichs, Terry, Lu, Wei-Yang, Field, R., Neilsen, M., "Validation of a Nonlinear Aluminum Honeycomb Constitutive Model for Impact Analyses", Proceedings of the IMAC XXV, A Conference on Structural Dynamics, Kissimmee, FL, Feb. 2005.
7. Carne, T.G., Neilsen, M.K., and Stasiunas, E.C., "Experimental and Analytical Validation of a Computationally Developed Orthotropic Constitutive Model," Proceedings of IMAC XXI, A Conference on Structural Dynamics, Kissimmee, FL, Feb. 2003.
8. Jones, R. M., Mechanics of Composite Materials, Scripta Book Co., 1975.
9. Koteras, J.R., Gullerud, A.S., "Presto User's Guide Version 1.05", SAND Report, SAND2003-1089, Sandia National Laboratories, Albuquerque, NM, April 2003.
10. Hinnerichs, Terry, Lu, Wei-Yang, Carne, Thomas G., et al., "Characterization of Aluminum Honeycomb and Experimentation for Model Development and Validation, Volume II: Honeycomb Experimentation for Model Development and Validation", Sandia National Laboratories, Albuquerque, NM 87185, SAND2006-4455, Sep 2006.
11. Lu, Wei-Yang, Friction Test Report, internal memo, Sandia National Laboratories, Livermore, CA, May 2006.